JCB Article

Mmm2p, a mitochondrial outer membrane protein required for yeast mitochondrial shape and maintenance of mtDNA nucleoids

Matthew J. Youngman, Alyson E. Aiken Hobbs, Shawn M. Burgess, Maithreyan Srinivasan, and Robert E. Jensen

Department of Cell Biology, The Johns Hopkins University School of Medicine, Baltimore, MD 21205

The mitochondrial outer membrane protein, Mmm1p, is required for normal mitochondrial shape in yeast. To identify new morphology proteins, we isolated mutations incompatible with the *mmm1-1* mutant. One of these mutants, *mmm2-1*, is defective in a novel outer membrane protein. Lack of Mmm2p causes a defect in mitochondrial shape and loss of mitochondrial DNA (mtDNA) nucleoids. Like the Mmm1 protein (Aiken Hobbs, A.E., M. Srinivasan, J.M. McCaffery, and R.E. Jensen. 2001. *J. Cell Biol*. 152:401–410.), Mmm2p is located in dot-like particles on the mitochondrial surface, many of which are adjacent to mtDNA nucleoids. While some of the Mmm2p-containing spots colocalize with those containing Mmm1p, at least some of Mmm2p is separate from Mmm1p. Moreover, while Mmm2p and Mmm1p both appear to be part of large complexes, we find that Mmm2p and Mmm1p do not stably interact and appear to be members of two different structures. We speculate that Mmm2p and Mmm1p are components of independent machinery, whose dynamic interactions are required to maintain mitochondrial shape and mtDNA structure.

Introduction

Mitochondria are ubiquitous organelles in eukaryotic cells that play key roles in a wide variety of cellular processes, ranging from energy production to aging (Attardi and Schatz, 1988). Mitochondria in different cell types differ not only in their size and number but also in their structure (Tandler and Hoppel, 1972). Although mitochondria in most cell types form long, thread-like organelles, in other cell types, a striking diversity of shapes can be seen. Despite the fact that mitochondria and their morphology have been studied for more than a century, the molecules and mechanisms that control the shape of mitochondria are just beginning to be elucidated.

The cellular components that mediate mitochondrial morphology are being revealed through the isolation and analysis of mutants in the yeast *Saccharomyces cerevisiae*. Mutants defective in mitochondrial shape have been isolated by screening yeast mutants by fluorescence microscopy (McConnell and Yaffe, 1992; Burgess et al., 1994; Hermann et al., 1997; Sesaki and Jensen, 1999; Dimmer et al., 2002). Using this approach, three mitochondrial outer membrane proteins, Mmm1p, Mdm10p, and Mdm12p, have been identified and characterized. In *mmm1*, *mdm10*, and *mdm12* mutants, the elongated and branched structure of mitochondrial tubules is no longer seen (Burgess et al., 1994; Sogo and Yaffe, 1994; Berger et al., 1997). Instead, mitochondria appear as a few large, spherical organelles. Mmm1p, Mdm10p, and Mdm12p are also required for stability of the mitochondrial DNA (mtDNA). In yeast cells, the mitochondrial genome is present in multiple copies, and mtDNA is organized into ∼10–20 separate DNA–protein complexes called nucleoids (Miyakawa et al., 1984). In *mmm1*, *mdm10*, and *mdm12* disruption strains, mtDNA is frequently lost and the mutant strains have growth defects on nonfermentable medium (Burgess et al., 1994; Sogo and

A.E. Aiken Hobbs and S.M. Burgess made equal contributions to this work.

The online version of this article contains supplemental material.

Address correspondence to Robert E. Jensen, Department of Cell Biology, Johns Hopkins University School of Medicine, 725 N. Wolfe St., Baltimore, MD 21205. Tel.: (410) 955-7291. Fax: (410) 955-7293. email: rjensen@jhmi.edu

S.M. Burgess's present address is National Human Genome Research Group, Building 50, Room 5537, 50 South Dr., MSC 8004, Bethesda, MD 20892-8004.

M. Srinivasan's present address is 454 Life Sciences, 20 Commercial St., Bradford, CT 06405.

Key words: mitochondrial morphology; mtDNA nucleoids; outer membrane protein

Abbreviations used in this paper: DIC, differential interference contrast; mtDNA, mitochondrial DNA; RFP, red fluorescent protein; TEV, tobacco etch virus.

Yaffe, 1994; Berger et al., 1997). In addition to their role in mitochondrial shape and mtDNA stability, Mmm1p, Mdm10p, and Mdm12p may also function in mitochondrial segregation. The altered organelles in *mmm1*, *mdm10*, and *mdm12* mutants are not efficiently transmitted from mother to daughter during cytokinesis (Burgess et al., 1994; Sogo and Yaffe, 1994; Berger et al., 1997).

Mmm1p appears to be located in several punctate structures on the mitochondrial surface. An Mmm1p-GFP fusion protein is seen in several dot-like structures along mitochondrial tubules, and the Mmm1p-containing spots are adjacent to a subset of mtDNA nucleoids (Aiken Hobbs et al., 2001). Our observations that the outer membrane Mmm1 protein was next to matrix-localized mtDNA raised the possibility that Mmm1p was located at contact sites, regions where the outer membrane is in close apposition with the inner membrane. Support for this idea comes from mitochondrial fractionation studies. In particular, mitochondrial membrane vesicles containing Mmm1p sediment in fractions intermediate in density between outer and inner membrane vesicles (Aiken Hobbs et al., 2001).

Using a genetic approach for potential Mmm1p-interacting proteins, we have identified a new mitochondrial outer membrane protein, called Mmm2p. We find that Mmm2p is required for maintenance of mitochondrial shape and mtDNA structure, Mmm2p is located in discrete spots next to mtDNA nucleoids, and that Mmm2p and Mmm1p often colocalize.

Results

Identification of Mmm2p, a potential Mmm1p-interacting protein

To find new genes required for mitochondrial shape, we used a genetic screen to identify mutations that are synthetically lethal in combination with *mmm1-1*. *mmm1-1* mutants are temperature sensitive for their mitochondrial morphology and for growth on nonfermentable carbon sources (Burgess et al., 1994). *ade2 mmm1-1* strain YSB105 was transformed with pSB201, a plasmid that carries the wild-type *MMM1* gene, as well as the *ADE2* and *URA3* genes. After chemical mutagenesis, colonies were screened for *mmm1-1* synthetic lethal mutants using a plasmid-shuffle scheme (Sikorski and Boeke, 1991). Specifically, we screened for colonies that were able to grow on lactate-containing medium at 24°C, only if they also carried the *MMM1-ADE2-URA3*–containing plasmid. 16 mutants unable to live without the plasmid were isolated, and one of these mutants, SB8, was crossed to a wild-type strain, and after selecting for plasmid loss, the diploid was sporulated and meiotic segregants were analyzed. SB8 was found to contain two unlinked mutations affecting cell growth and mitochondrial morphology: the original *mmm1-1* lesion and a new mutation, called *mmm2-1*. *mmm1-1 mmm2-1* double mutants failed to grow on nonfermentable medium, even at 24°C. On glucose medium, *mmm1-1 mmm2-1* cells grew extremely slowly and showed a mitochondrial morphology defect similar to the *mmm1*Δ disruption mutant (Fig. 1). While *mmm1-1* cells are temperature sensitive for their mitochondrial shape, *mmm1-1 mmm2-1* double mutants contained aberrant mitochondria at both 24°C and 37°C. Segregants carrying *mmm2-1* alone (unpublished data), or *mmm1-1 mmm2-1* double mutants carrying the *MMM1* plasmid (Fig. 1), showed no growth defect or mitochondrial shape alteration on glycerol/ethanol-containing medium at 24°C or 37°C. Our results show that SB8 contains a new mutation called *mmm2-1,* which is lethal in combination with *mmm1-1* when cells are grown on nonfermentable medium.

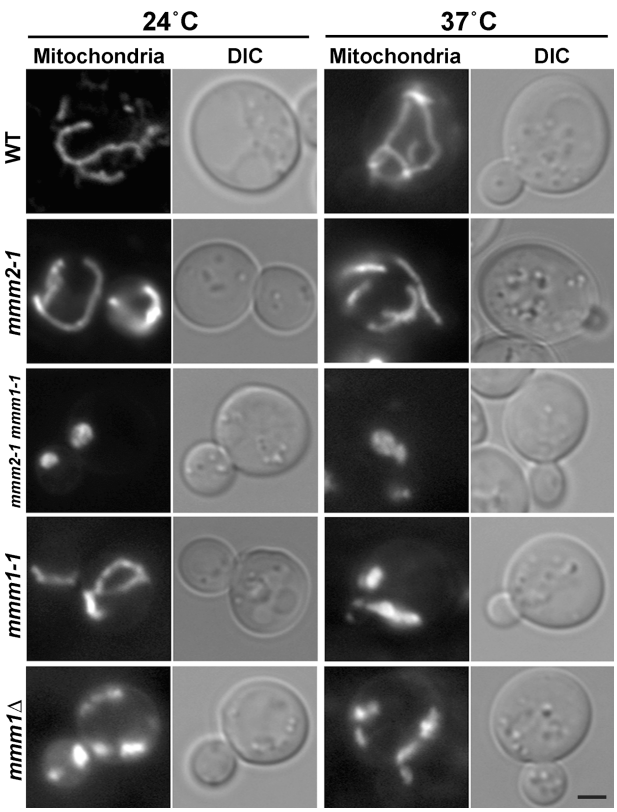

Figure 1. **The combination of *mmm2-1* and *mmm1-1* disrupts mitochondrial shape.** Wild-type strain YPH250, *mmm1-1* strain YSB105, *mmm1-1 mmm2-1* strain SB9, *mmm1-1 mmm2-1* strain SB9 carrying the *MMM1* plasmid, pSB201, and *mmm1*Δstrain YSB120 were grown at 24°C or 37°C, stained with Mitofluor 589 (Mitochondria) and then examined by fluorescence and DIC microscopy. Representative images are shown. Bar, 3 μm.

To identify the *mmm1-1* synthetic lethal defect in SB8, cells were transformed with a genomic DNA library, and colonies were screened for rescue of the *MMM1-ADE2-URA3* plasmid dependence of *mmm1-1 mmm2-1* cells. One transformant was found to carry a library plasmid with a genomic DNA insert from chromosome VII. The ORF that encodes the *mmm2-1* complementing activity was shown to be YGL219c (see Materials and methods). Mmm2p is a novel, 52-kD protein. Although no clear cognates are found in higher eukaryotic cells, we note that very similar proteins are found in other fungi, such as *Schizosaccharomyces pombe* (49% similar; 27% identical) and *Neurospora crassa* (52% similar; 31% identical). Although Mmm2p has no obvious α-helical transmembrane stretches, Mmm2p is predicted to contain several β-sheet regions. We also note that *MMM2* is allelic with the *MDM34* gene, which was identified in a screen of yeast deletion mutants for those with mitochondrial shape and distribution defects (Dimmer et al., 2002).

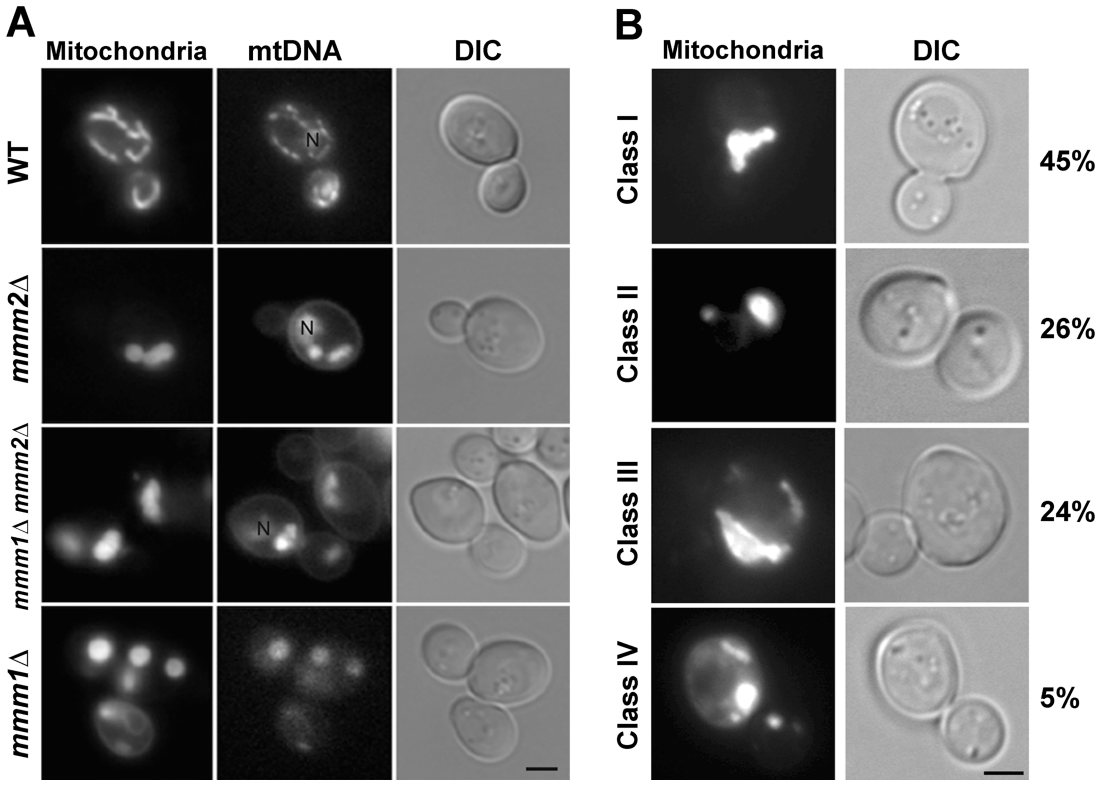

Figure 2. **Mmm2p is required for mitochondrial shape and maintenance of mtDNA nucleoids.** (A) Mitochondria and mtDNA in *mmm2*Δ, *mmm1*Δ, and *mmm1*Δ *mmm2*Δ cells. Wild-type strain MY4, *mmm1*Δ strain MY1, *mmm2*Δ strain MY2, and *mmm1*Δ *mmm2*Δ strain MY3 were grown in glycerol/ethanol medium, stained with Mitofluor 589 (Mitochondria) or DAPI (mtDNA), and then examined by DIC and fluorescence microscopy. Representative images of cells are shown. N, staining of the nucleus by DAPI. Bar, 3 μm. (B) Classification of *mmm2*Δ phenotypes. *mmm2*Δ strain MY2 was stained with $DiOC_6$ and then examined by DIC and fluorescence microscopy. Cells were sorted into four groups based on their mitochondrial appearance. Class I, distorted and sausage-shaped mitochondria; Class II, spherical-shaped mitochondria; Class III, sheet-like mitochondria; Class IV, a mixture of distorted and spherical-shaped mitochondria. A representative from each group is shown, and the percentage of cells (out of 107 total cells examined) in each category is indicated to the right of each image. Bar, 3 μm.

Mmm2p is required for normal cell growth, mtDNA nucleoid structure, and mitochondrial shape

To explore the function of Mmm2p, we disrupted *MMM2* in yeast cells and compared the *mmm2*Δ mutant with cells lacking Mmm1p (*mmm1*Δ) and with *mmm2*Δ *mmm1*Δ double mutants. While all the strains grew on glucose-containing medium, we found that *mmm2*Δ cells and *mmm2*Δ *mmm1*Δ double mutants grew slowly, with a doubling time approximately four- to sixfold greater than wild-type cells (unpublished data). *mmm1*Δ cells were less defective in their growth than *mmm2*Δ cells (approximately twofold increase in doubling time). While wild-type cells readily grew when they were struck from glucose-containing medium onto plates with glycerol and ethanol as the carbon source, *mmm2*Δ, *mmm1*Δ, and *mmm2*Δ *mmm1*Δ cells were initially deficient in their growth. No colonies were seen after 3 or 4 d of incubation. However, we found that *mmm2*Δ, *mmm1*Δ, and *mmm2*Δ *mmm1*Δ mutants could eventually grow on the nonfermentable medium, and single colonies were clearly visible after 10–14 d of incubation. Moreover, once these cells had adapted to the nonfermentable medium, they could immediately grow upon transfer to new glycerol/ethanol plates, albeit at a slower rate than wild-type cells (unpublished data).

Our observations suggest that *mmm2*Δ, *mmm1*Δ, and *mmm2*Δ *mmm1*Δ mutants are defective in their growth on nonfermentable medium because they lack sufficient mtDNA and normal nucleoid structure. When the amount of mtDNA was determined by Southern blotting, we found that *mmm2*Δ, *mmm1*Δ, and *mmm2*Δ *mmm1*Δ cells grown on glucose medium contain significantly less mtDNA than the wild-type parent (Table I). However, after the *mmm2*Δ, *mmm1*Δ, and *mmm2*Δ *mmm1*Δ mutants adapted to growth on glycerol/ethanol medium, they contained at least as much mtDNA as wild-type cells. Examination of glycerol/ethanol-grown cells after DAPI staining showed that *mmm2*Δ, *mmm1*Δ, and *mmm2*Δ *mmm1*Δ mutants con-

Table I. **Percent mtDNA levels in mutants on YEPD vs. YEPGE media as compared with wild type**

	Carbon source	
Strain	**YEPD**	**YEPGE**
Wild type	100	100
*mmm2*Δ	16 ± 0.5	180 ± 23.7
*mmm2*Δ *mmm1*Δ	38 ± 18.3	157 ± 19.5
*mmm1*Δ	12 ± 3.9	161 ± 13.8

Total DNA was isolated from a tetratype tetrad grown in either YEPD or YEPGE, Southern blotted, and probed with ^{32}P-labeled mitochondrial *COX2* gene. After normalization to the levels of hybridized nuclear-encoded *TIM23* gene, relative amounts of mtDNA (*COX2* signal) are compared.

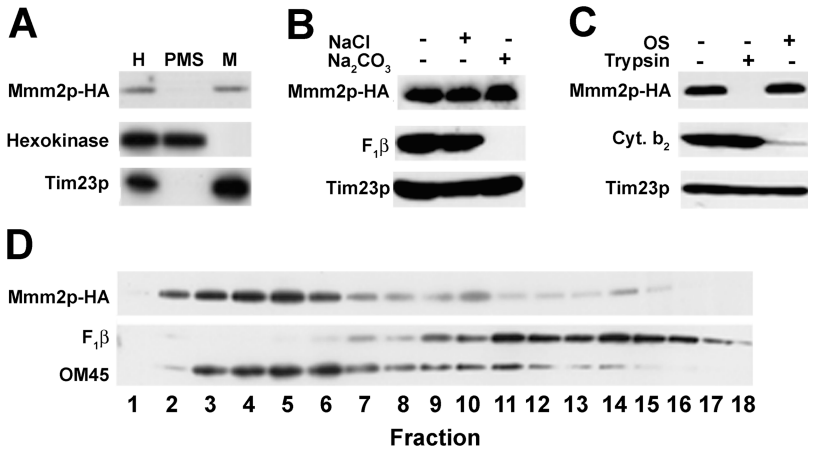

Figure 3. **Mmm2p is a mitochondrial outer membrane protein.** (A) Mmm2p-HA is a mitochondrial protein. Strain RJ892, expressing Mmm2p-HA, was grown and homogenized (H) and then separated into a mitochondrial pellet (M) and a post-mitochondrial supernatant (PMS) by centrifugation. Aliquots of the fractions were analyzed by SDS-PAGE and Western blotting, using antibodies to the HA epitope (Mmm2p-HA), or antiserum to the mitochondrial protein, Tim23p, or to the cytosolic hexokinase protein. (B) Mmm2p is an integral membrane protein. Mitochondria from cells expressing Mmm2p-HA were incubated with buffer, 1.5 M sodium chloride, or 0.1 M sodium carbonate. After centrifugation, membrane pellets were analyzed by SDS-PAGE and Western blotting with HA antibodies (Mmm2p-HA), or antiserum to Tim23p or the β subunit of the F_1-ATPase ($F_1\beta$). (C) The COOH terminus of Mmm2p faces the cytosol. Mmm2p-HA mitochondria were incubated in the presence or absence of 100 μg/ml trypsin. In one aliquot of mitochondria, the outer membrane was disrupted by osmotic shock (OS). After centrifugation, mitochondrial proteins were analyzed by Western blotting using HA antibodies (Mmm2p-HA), or antiserum to Tim23p or cytochrome b_2 (Cyt. b_2). (D) Mmm2p is located in the outer membrane. Mmm2p-HA–containing mitochondria were sonicated, and membrane vesicles were loaded onto a sucrose density gradient. Fractions were collected and analyzed by Western blotting, using HA antibodies (Mmm2p-HA) or antiserum to the OM45 and F1β proteins. Fraction 1 corresponds to the top of the gradient.

tained mtDNA but lacked discernible nucleoids (Fig. 2 A). While wild-type cells contained normal nucleoids, seen as 10–20 small DAPI-staining dots, mtDNA in *mmm2*Δ, *mmm1*Δ, and *mmm2*Δ *mmm1*Δ cells was diffuse and disorganized. Similarly disorganized mtDNA was seen in *mmm2*Δ, *mmm1*Δ, and *mmm2*Δ *mmm1*Δ mutants grown on glucose medium, but much less mtDNA was apparent (unpublished data). Our results thus indicate that Mmm2p and Mmm1p are required for normal nucleoid structure, and at least on glucose medium, Mmm2p and Mmm1p are also necessary for normal levels of mtDNA.

In addition to their defects in mtDNA structure, we found that *mmm2*Δ, *mmm1*Δ, and *mmm2*Δ *mmm1*Δ cells contained altered mitochondrial shapes (Fig. 2 A). While wild-type cells contained 5–10 tubular-shaped mitochondria, the mitochondria in both *mmm2*Δ and *mmm1*Δ cells were noticeably misshapen. Consistent with our previous studies (Burgess et al., 1994; Aiken Hobbs et al., 2001), we found that most of the *mmm1*Δ cells contained two or three large mitochondria that were either round or slightly oblong in shape. Compared with *mmm1*Δ cells, the *mmm2*Δ mutant showed a greater variation in the structures of their aberrant mitochondria (Fig. 2 B). While about a quarter of the *mmm2*Δ cells contained two or three spherical-shaped mitochondria similar to those in *mmm1*Δ cells (Fig. 2 B, Class II), about half of the cells contained one or two mitochondria more irregular in shape, which we have termed "distorted" or "sausage shaped" (Fig. 2 B, Class I). A small fraction of the cells (~5%) had a mixture of both spherical and distorted shapes (Fig. 2 B, Class IV). In ~24% of the *mmm2*Δ cells, the mitochondria exhibited more of a sheet-like appearance (Fig. 2 B, Class III). We also found that the mitochondrial alterations in the *mmm2*Δ *mmm1*Δ double mutant are more like those in cells lacking only Mmm2p than in cells lacking only Mmm1p (Fig. 2 A).

While the shape of mitochondria in *mmm1*Δ cells was more uniform than in the *mmm2*Δ mutant, we did notice that other factors, such as temperature, carbon source, and strain background, could have subtle effects on the altered mitochondrial shapes seen in both *mmm2*Δ and *mmm1*Δ cells (unpublished data). In particular, we found that if *mmm2*Δ and *mmm1*Δ cells lost their mtDNA, they contained more uniformly round mitochondria than cells with mtDNA. However, the lack of mtDNA is not solely responsible for mitochondrial shape, since aberrant structures are clearly present in *mmm2*Δ and *mmm1*Δ cells with or without mtDNA. Thus, our observations show that Mmm2p, like Mmm1p, is required for normal mitochondrial shape.

We find that the requirement for Mmm2p appears to be limited to mitochondria. As mitochondrial structure in yeast is dependent upon the actin cytoskeleton (Drubin et al., 1993) and can be affected by alterations in ER structure

Table II. **Colocalization of Mmm2p with mtDNA and Mmm1p**

	Associates with		
Reference marker	**mtDNA**	**Mmm1p-GFP**	**Mmm2p-GFP**
Mmm2p-GFP/RFP (3–7)[a]	58% (n = 181)[b]	71% (n = 358)[b]	---
mtDNA (10–20)[a]	---	52% (n = 356)[b,c]	19% (n = 288)[b]
Mmm1p-GFP (6–11)[a]	87% (n = 213)[b,c]	---	33% (n = 779)[b]

[a]Average number of structures/cell.
[b]Total number of structures analyzed is given in parentheses.
[c]As determined in Aiken Hobbs et al., 2001.

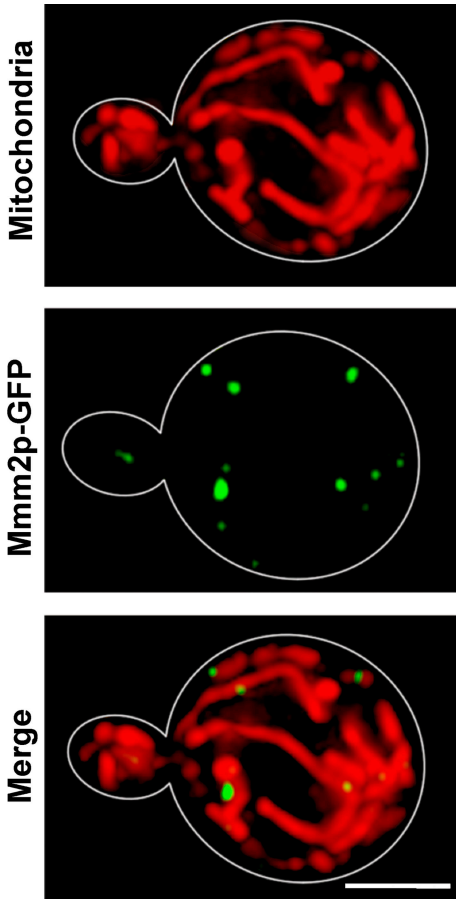

Figure 4. **Mmm2p-GFP localizes to small spots along mitochondrial tubules.** *mmm2*Δ strain RJ713, expressing the Mmm2p-GFP fusion protein from pAAH13, was stained with Mitotracker Red and examined by deconvolution microscopy. A total of 15 images were taken at 0.2-μm intervals in the z-axis, deconvolved, and then compressed into a single image. Mitotracker Red (Mitochondria), Mmm2p-GFP, and merged images with both Mmm2p-GFP and Mitotracker Red are shown. Bar, 3 μm.

(Prinz et al., 2000), we asked if the distribution of actin or the organization of the ER was disrupted in cells lacking Mmm2p. As shown in Fig. S1 (available at http://www.jcb.org/cgi/content/full/jcb.200308012/DC1), no significant differences in actin or the ER were found in *mmm2*Δ, *mmm1*Δ, or *mmm2*Δ *mmm1*Δ cells, as compared with wild type.

Mmm2p is located in the mitochondrial outer membrane

We constructed an Mmm2p-HA fusion protein by inserting an influenza HA epitope at the COOH terminus of Mmm2p and then integrating this construct into the *MMM2* locus. As cells expressing Mmm2p-HA as the sole source of Mmm2 protein show no cell growth or mitochondrial morphology defect, we conclude that the Mmm2p-HA fusion protein is fully functional. Cell fractionation studies indicate that Mmm2p is a mitochondrial protein (Fig. 3 A). Yeast cells expressing the Mmm2p-HA fusion protein were homogenized and separated into a mitochondrial pellet and a post-mitochondrial supernatant by centrifugation. We found that Mmm2p was located in the mitochondrial fraction along with the mitochondrial Tim23 protein, while a negligible amount of Mmm2p was found in the supernatant with the cytosolic hexokinase protein. Mmm2p, like many outer membrane proteins, does not appear to contain a typical NH_2-terminal presequence and contains internal mitochondrial targeting information. When mitochondria were disrupted by osmotic shock and sonication, Western blots showed that Mmm2p is an integral protein. Virtually all of Mmm2p-HA was found in the pellet fraction after the mitochondria were treated with salt or alkalai, identical to the inner membrane Tim23 protein (Fig. 3 B). In contrast, the peripherally associated β subunit of the F1-ATPase ($F_1\beta$) was quantitatively removed by carbonate treatment. As Mmm2p lacks α-helical transmembrane segments, it is likely that Mmm2p resides in the membrane via β-sheet conformations similar to those predicted for other outer membrane proteins, such as Mdm10p (Sogo and Yaffe, 1994) and porin (Forte et al., 1987).

We found that the COOH-terminal HA tag of the Mmm2p-HA fusion protein was accessible to trypsin digestion in intact mitochondria, suggesting that Mmm2p is an outer membrane protein (Fig. 3 C). Cytochrome b_2, which is located in the intermembrane space, and the inner membrane Tim23 protein were not digested by the protease, showing that our mitochondria were intact. We also found that Mmm2p cofractionates with outer membrane proteins in vesicles prepared by sonication of Mmm2p-HA–containing mitochondria. On sucrose density gradients, Mmm2p migrated with OM45, a protein located in the outer membrane, and not with the $F_1\beta$ protein, an inner membrane protein (Fig. 3 D).

Mmm2p is localized in discrete spots on mitochondria, often next to mtDNA nucleoids and Mmm1p

We find that Mmm2p, like Mmm1p (Aiken Hobbs et al., 2001), is located in a punctate distribution along mitochondrial tubules. Mmm2p was localized in live cells by expressing GFP fused to the COOH terminus of Mmm2p (Mmm2p-GFP), a fully functional fusion protein. When yeast cells expressing Mmm2p-GFP were examined by fluorescence microscopy (Fig. 4), we found approximately seven Mmm2p-GFP–containing dots per cell (181 Mmm2-GFP dots in 25 total cells). Mother cells tended to contain more Mmm2p-GFP particles than daughter buds, but this difference may simply be due to the smaller size of the daughter cell or their lower mitochondrial content. 3D reconstructions showed that each of the Mmm2p-GFP structures was located on a mitochondrial tubule.

When the mtDNA of Mmm2-GFP cells was stained with DAPI, we found that about half of Mmm2p was next to nucleoids (Fig. 5; see Table II for quantitation). In most of our merged images, we note that the Mmm2p-GFP and nucleoids were seen as twin, dot-like structures, one red and one green, and do not strictly overlap or colocalize. Occasionally, a single yellow dot was seen, which presumably represented a pair of dots viewed from the top or bottom, instead of from the side. Since there appears to be many more nucleoids than Mmm2p-GFP structures, we found that the majority of mtDNA particles did not associate with Mmm2p-

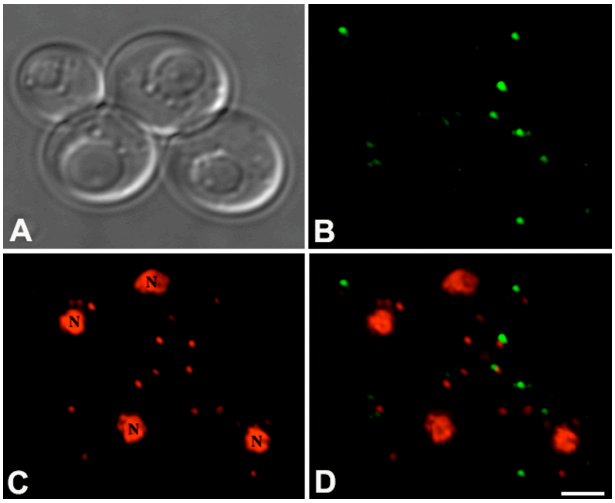

Figure 5. **Mmm2p is adjacent to a subset of mtDNA nucleoids.** *mmm2*Δ strain RJ713, expressing the Mmm2p-GFP fusion protein from pAAH13, was stained with DAPI and examined by deconvolution microscopy. Each image represents a flattened, deconvolved composite of 15 images. (A) DIC, (B) Mmm2p-GFP, (C) DAPI, (D) merged images showing both Mmm2p-GFP and DAPI. DAPI staining of the yeast nucleus (N) is indicated. Bar, 3 μm.

GFP (Table II). Consistent with previous studies (Aiken Hobbs et al., 2001), we found that Mmm1p-GFP was next to nucleoids >85% of the time (Table II).

To examine the association between Mmm2p and Mmm1p, we constructed a yeast strain expressing a fusion between Mmm2p and the red fluorescent protein (Mmm2p-RFP) and Mmm1p-GFP. We found that Mmm2p-RFP and Mmm1p-GFP were each located in punctate spots on mitochondria, although it appeared that Mmm1p-containing complexes were more abundant than Mmm2p particles (Fig. 6). Each cell contained ~6–11 Mmm1p-GFP dots compared with ~3–7 Mmm2p-RFP dots. We found that the Mmm2p-RFP and Mmm1p-GFP structures frequently, but not always, overlapped. While about two thirds of the Mmm2p-RFP colocalized with Mmm1p-GFP, we did find that a significant amount of the Mmm2p-RFP was distinct from Mmm1p-GFP (see Table II for quantitation). Since there were more Mmm1p-GFP dots than Mmm2p-RFP dots in each cell, it was not surprising that a smaller percentage of Mmm1p-GFP colocalized with Mmm2p-RFP. Our results indicate that Mmm2p and Mmm1p-containing complexes can be found either together or separate in the cell, and raise the possibility that the interaction between Mmm2p and Mmm1p is dynamic.

Mmm2p is required for normal Mmm1p levels, while Mmm1p is necessary for the punctate distribution of Mmm2p

When *mmm1*Δ cells expressing an Mmm2p-GFP fusion protein were examined by fluorescence microscopy (Fig. 7 A), Mmm2p was found uniformly distributed all over the large, spherical mitochondria of *mmm1*Δ cells, instead of the punctate distribution of Mmm2p-GFP seen on mitochondrial tubules in wild-type cells. Western blots showed that normal amounts of Mmm2p are present in mitochondria

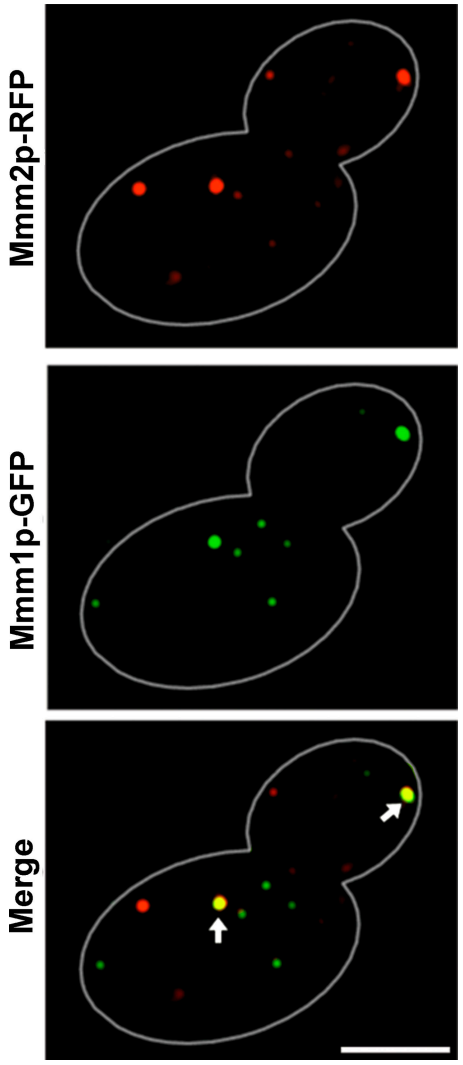

Figure 6. **Mmm2p colocalizes with a fraction of Mmm1p.** Strain AAH4, which expresses Mmm1p-GFP from the chromosomal *MMM1::GFP* gene and Mmm2p-RFP from pMY3, was examined by deconvolution microscopy. A single image containing 15 deconvolved and compressed images is shown. Mmm2p-RFP, Mmm1p-GFP, and merged images with both Mmm1p-GFP and Mmm2p-RFP are shown. Arrows indicate an example of colocalization of Mmm2p-RFP and Mmm1p-GFP. The cell outline, as seen by phase contrast, is shown by white lines. Bar, 3 μm.

isolated from *mmm1*Δ cells (Fig. 7 C). Thus, Mmm1p appears to be required to organize Mmm2p into the dot-like structures on mitochondria. In contrast, *mmm2*Δ cells contain little or no Mmm1p (Fig. 7 C). Quantitation of Western blots indicates that *mmm2*Δ mitochondria contain at least 10-fold less Mmm1p than wild-type mitochondria. Fluorescence microscopy also showed that little or no Mmm1p-GFP is seen in *mmm2*Δ cells (Fig. 7 B). Our results therefore suggest that Mmm2p plays a role in the synthesis, import, or stability of Mmm1p.

Mmm2p and Mmm1p are located in large, but separate, complexes

To further examine the relationship between Mmm2p and Mmm1p, we solubilized mitochondria with digitonin-con-

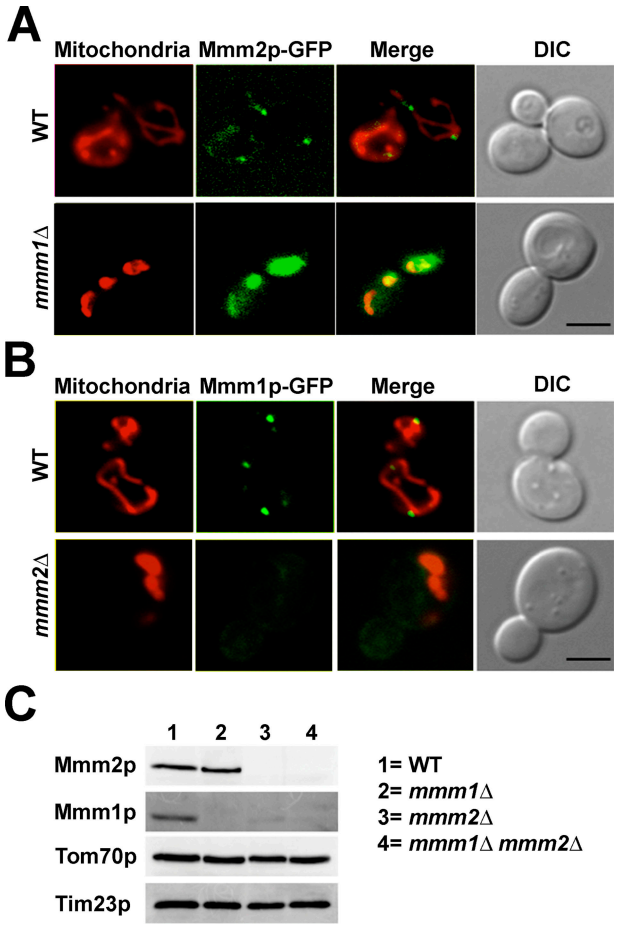

Figure 7. **Mmm1p is necessary for the punctate distribution of Mmm2p, while Mmm2p is required for normal Mmm1p levels.** (A) Wild-type strain MY4 and *mmm1*Δ strain MY5, each expressing Mmm2p-GFP from chromosomal *MMM2::GFP*, were stained with Mitofluor 589 and examined by DIC and fluorescence microscopy. Mitofluor 589 (Mitochondria), Mmm2p-GFP, merged images with both Mmm2p-GFP and Mitofluor 589, and DIC images are shown. Bar, 3 μm. (B) Wild-type strain SS12 and *mmm2*Δ strain AAH4, each carrying a chromosomal version of *MMM1::GFP*, were stained with Mitofluor 589 and examined by DIC and fluorescence microscopy. Mitofluor 589 (Mitochondria), Mmm1p-GFP, merged images with both Mmm1p-GFP and Mitofluor 589, and DIC images are shown. Bar, 3 μm. (C) Mitochondria (100 μg) were isolated from isogenic wild-type, *mmm1*Δ, *mmm2*Δ, and *mmm1*Δ *mmm2*Δ cells and Western blotted using antibodies to Mmm2p, Mmm1p, Tom70p, an outer membrane protein, and Tim23p, an inner membrane protein.

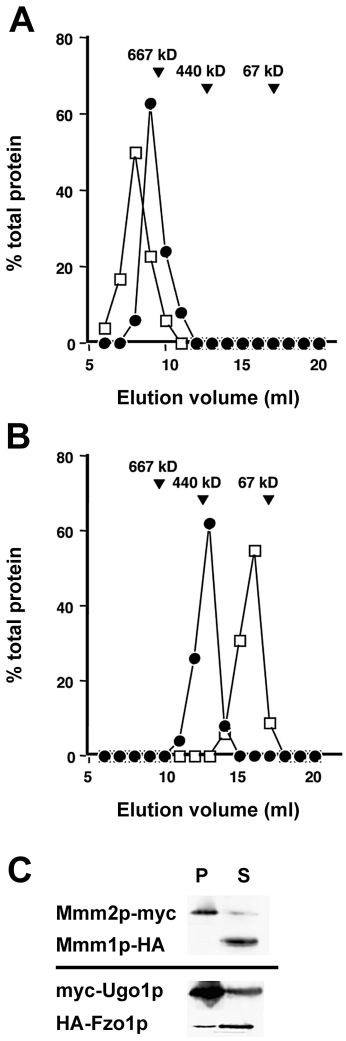

Figure 8. **Mmm2p and Mmm1p are in large, but separate, membrane complexes.** (A) Gel filtration analysis of Mmm2p and Mmm1p. Mitochondria were solubilized in digitonin-containing buffer and loaded onto a gel filtration column. Aliquots from each fraction were analyzed by Western blotting using antiserum to Mmm2p (open squares) or affinity-purified antibodies to Mmm1p (filled circles). After quantitation by densitometry, protein amounts are shown as a percent of total Mmm1p or Mmm2p proteins in the extract. (B) Analysis of the same column fractions as in A, but using antiserum to Tom40p (filled circles) or Tim23p (open squares). Molecular masses (shown above the graphs) were estimated by running protein calibration standards under identical conditions. (C) Mmm2p and Mmm1p do not coimmunoprecipitate. Mitochondria isolated from strain RJ1719, expressing Mmm1p-HA and Mmm2p-myc fusion proteins, or from strain RJ1302, expressing HA-Fzo1p and myc-Ugo1p fusion proteins, were solubilized in Triton X-100 and subjected to immunoprecipitation using antibodies to the myc epitope. Equal aliquots from the pellet (P) and supernatant (S) fraction were Western blotted using antibodies to either the HA or myc epitopes.

taining buffer and separated proteins by detergent gel filtration. Mmm2p and Mmm1p both appear to reside in sizeable complexes, eluting from the column before the largest molecular mass standard, thyroglobulin (667 kD; Fig. 8 A). However, the Mmm2p- and Mmm1p-containing structures do not appear to strictly cofractionate. The peak fraction of Mmm2p appears to elute one or two fractions earlier than the peak of Mmm1p, suggesting that the Mmm1p- and Mmm2p-containing complexes may be distinct. Consistent with previous studies (Berthold et al., 1995; Dekker et al., 1996, 1997), we find Tom40p, a mitochondrial outer membrane protein, in a complex of ~400 kD and the inner membrane protein, Tim23p, in an ~100-kD complex (Fig. 8 B).

Coimmunoprecipitation experiments also indicate that Mmm2p and Mmm1p do not stably interact (Fig. 8 C). Under conditions where Mmm2p was efficiently precipitated from Triton X-100 or digitonin extracts of mitochondrial proteins, Mmm1p did not precipitate with Mmm2p. However, known mitochondrial membrane complexes could be detected by our procedures, since Ugo1p and Fzo1p, two outer membrane proteins required for mitochondrial fusion

(Fig. 8 C; Sesaki et al., 2003), were shown to coimmunoprecipitate. Therefore, we suggest that the association of Mmm2p and Mmm1p is weak or transient.

Discussion

To find new proteins required for mitochondrial shape, we isolated mutations that exacerbated the growth defect of the temperature-sensitive *mmm1-1* mutant and identified a new gene, called *MMM2*. While *mmm1-1* cells can grow at the permissive temperature on nonfermentable medium, we find that *mmm1-1 mmm2-1* cells cannot. Mutants that are incompatible with each other, so-called synthetic lethal mutants, often identify proteins that interact or whose gene products act in the same pathway (Basson et al., 1987; Bender and Pringle, 1991). A number of observations suggest that the Mmm2 and Mmm1 proteins both play a role in mitochondrial shape and mtDNA nucleoid structure: (1) lack of either protein results in a dramatic loss of mitochondrial shape and mtDNA organization, (2) high levels of *MMM2* partially rescue the morphology defect of *mmm1*Δ cells (unpublished data), (3) both proteins are located in the mitochondrial outer membrane, (4) Mmm2p and Mmm1p are each located in small particles on the mitochondrial surface, next to a subset of mtDNA nucleoids, (5) a significant fraction of the Mmm2p-containing dots colocalize with Mmm1p-containing structures, and (6) Mmm2p and Mmm1p are required for each other's distribution in the cell.

Although the distributions of Mmm2p and Mmm1p seem remarkably similar, we suggest that the Mmm2p–Mmm1p interaction is transient and dynamic. In particular, while the fluorescence of Mmm2p-GFP and Mmm1p-RFP sometimes overlapped, much of the time the Mmm2p- and the Mmm1p-containing structures were distinct. Moreover, while Mmm2p and Mmm1p are both mitochondrial outer membrane proteins, they appear to differ in their location in the outer membrane. Our previous work suggested that Mmm1p resides at contact sites, or connections between the mitochondrial outer and inner membranes (Aiken Hobbs et al., 2001). When mitochondrial membrane vesicles were run on sucrose gradients, Mmm1p migrated in fractions intermediate in density between the outer and inner membrane fractions. In contrast, we find that Mmm2p behaves like a typical outer membrane protein in our fractionation studies. Thus, Mmm2p does not appear to be stably located at contact sites along with Mmm1p. Gel filtration and immunoprecipitation studies also indicate that any Mmm2p–Mmm1p interaction may be short-lived or indirect.

While Mmm2p and Mmm1p do not firmly associate in mitochondrial extracts, we find that each protein appears to be part of a large membrane complex. Gel filtration analysis of digitonin-solubilized mitochondria indicates that Mmm1p migrates in a structure with a molecular mass of >667 kD. Mmm2p appears to be in a complex somewhat larger than Mmm1p, with the peak of Mmm2p eluting off the column one or two fractions ahead of the Mmm1p-containing peak. Studies are underway to further characterize these two complexes with regards to their actual sizes and their subunit compositions.

In addition to their role in mitochondrial shape, Mmm2p and Mmm1p are required for maintenance of mtDNA nucleoid structure. In *mmm2*Δ and *mmm1*Δ cells, mtDNA is diffuse and disordered, instead of being organized into the punctate DNA–protein complexes seen in wild-type cells. Thus, cells lacking Mmm2p and Mmm1p are surprisingly similar to mutants defective in mtDNA-binding proteins required for nucleoid structure, such as Abf2p (Newman et al., 1996). When transferred from glucose medium to nonfermentable medium, both *mmm2*Δ and *mmm1*Δ mutants were defective in their growth. mtDNA levels in *mmm2*Δ and *mmm1*Δ cells grown on glucose were much lower than in wild-type cells, explaining the growth defect on the glycerol/ethanol medium. After longer incubation times on nonfermentable medium, both *mmm2*Δ and *mmm1*Δ cells were eventually able to grow, and an increase in the amount of mtDNA was seen in these cells. We also found that mtDNA was less stable in both *mmm2*Δ and *mmm1*Δ cells. *mmm1*Δ mutants lose their mtDNA more frequently than *mmm2*Δ cells, but in both cases, mtDNA loss appears to be stochastic and influenced by other factors, such as strain background and temperature. We suggest that Mmm2p and Mmm1p are both necessary to maintain the organization of mtDNA in nucleoids, and argue that the loss of mtDNA is a secondary consequence of defects in Mmm2p or Mmm1p function. Supporting this notion, our previous studies with the temperature-sensitive *mmm1-1* mutant showed that mtDNA nucleoid structure was lost within 90 min after cells were shifted to the restrictive temperature, but it took >2 d for cells to lose all of their mtDNA (Aiken Hobbs et al., 2001). Like mtDNA, bacterial chromosomes are attached to the membrane, and this connection is necessary for proper DNA replication, recombination, and segregation (Sherratt, 2003). Recently, it has been reported that Mmm1p is located next to the subset of mtDNA nucleoids undergoing DNA replication (Meeusen and Nunnari, 2003). However, as *mmm2*Δ and *mmm1*Δ mutants contain mtDNA and can transmit it to daughter cells, they do not appear to be defective in replication or segregation of mtDNA per se. Consequently, the role of Mmm2p and Mmm1p in mtDNA metabolism and nucleoid structure remains to be determined.

Since Mmm2p- and Mmm1p-containing structures are adjacent to nucleoids, and since mtDNA is attached to the mitochondrial membrane at discrete locations (Miyakawa et al., 1987; Azpiroz and Butow, 1993), we speculate that the loss of nucleoid structure in *mmm2* and *mmm1* mutants may be due to a defect in mtDNA attachment. Since our previous work suggested that Mmm1p was located in contact sites, we proposed that Mmm1p was connected to mtDNA via one or more inner membrane proteins (Aiken Hobbs et al., 2001). Candidates for some of these inner membrane proteins have recently been identified (Dimmer et al., 2002; Messerschmitt et al., 2003). Recently, Mmm1p has been reported to span both the outer and inner membranes, suggesting that Mmm1p may play a direct role in contact site formation and mtDNA attachment (Kondo-Okamoto et al., 2003). In particular, a unique tobacco etch virus (TEV) protease site, which was engineered near the NH_2 terminus of Mmm1p, was found to be processed by matrix-targeted TEV protease. However, in similar studies,

we found that a TEV site–containing Mmm1p fusion protein was inefficiently processed and required long inductions of the matrix-localized TEV for significant Mmm1p processing (unpublished data). Under these conditions, we found that the overproduced TEV protease cleaved TEV site–containing fusion proteins residing in the intermembrane space. We note that in Kondo-Okamoto et al. (2003), long inductions of matrix-targeted TEV were also needed for cleavage of the Mmm1p fusion protein, but much shorter inductions of TEV were used for the analysis of control proteins located in other mitochondrial locations. Consequently, the topology of Mmm1p remains uncertain. Mmm2p does not appear to permanently reside in contact sites and behaves like a typical outer membrane protein in fractionation studies. Thus, it is even more puzzling how Mmm2p interacts with mtDNA. One intriguing possibility is that Mmm2p is linked to mtDNA via Mmm1p-containing structures. While we find that most or all of Mmm1p is adjacent to nucleoids, only about half of Mmm2p is next to mtDNA. Perhaps the fraction of Mmm2p that colocalizes with Mmm1p is the same fraction that is next to mtDNA.

Mmm2p joins a growing list of proteins required for both mitochondrial shape and mtDNA structure or stability. For many of these proteins, their functions are known and their roles in mitochondrial morphology and mtDNA maintenance are probably indirect. For example, defects in mitochondrial fusion (Hermann et al., 1998; Sesaki and Jensen, 2001; Messerschmitt et al., 2003; Sesaki et al., 2003), mitochondrial protein turnover (Thorsness et al., 1993), or mitochondrial enzyme complex assembly (Paumard et al., 2002) can each lead to changes in mitochondrial shape and mtDNA loss. Double mutant analysis indicates that Mmm2p is not simply a new component of the mitochondrial fusion or division pathway. We observe that the mitochondria in *mmm2*Δ *dnm1*Δ and *mmm2*Δ *fzo1*Δ mutants appears more like those in *mmm2*Δ cells than in either the *dnm1*Δ or *fzo1*Δ mutant (see Fig. S2, available at http://www.jcb.org/cgi/content/full/jcb.200308012/DC1). Mitochondria in *mmm2*Δ and *mmm1*Δ mutants closely resemble the altered organelles seen in *mdm10*Δ and *mdm12*Δ mutants, suggesting that Mmm2p, Mmm1p, Mdm10p, and Mdm12p all play similar roles in mitochondrial dynamics. For example, mitochondria in *mmm2*Δ, *mdm10*Δ, and *mmm2*Δ *mdm10*Δ double mutants are virtually indistinguishable (Fig. S2). Like Mmm2p and Mmm1p, Mdm10p and Mdm12p have recently been found in small particles (Boldogh et al., 2003). Thus, further analysis of these proteins will likely provide important insights into the mechanism of mitochondrial and mtDNA morphogenesis.

Materials and methods

Yeast strains and relevant genotypes

Yeast strains used in this study are listed in Table S1 (available at http://www.jcb.org/cgi/content/full/jcb.200308012/DC1). *mmm2*Δ, *mmm1*Δ, and the *mmm1*Δ *mmm2*Δ double mutant were constructed by PCR-mediated gene replacement using the *HIS3* gene from plasmid pRS303 (Sikorski and Hieter, 1989) and the diploid strain RJ605 (formed by crossing FY833 to FY834). Oligonucleotides used for the *MMM1* disruption (oligos 313 and 314) and the *MMM2* disruption (oligos 154 and 155) are listed in Table S2 (available at http://www.jcb.org/cgi/content/full/jcb.200308012/DC1). After sporulation of the respective diploids, a *MATα mmm2::HIS3* strain and a *MATa mmm1::HIS3* were isolated and then crossed to each other. Isogenic wild-type strain MY4, *mmm2::HIS3* strain MY1, *mmm1::HIS3* strain MY2, and *mmm1::HIS3 mmm2::HIS3* strain MY3 were isolated after sporulation. An *mmm2::LEU2* disruption was constructed as follows. *mmm2::LEU2* was isolated after PstI digestion of pSB209 (see below) and was used to replace one of two copies of *MMM2* in *MATa/MATα leu2/leu2* diploid strain SM1060 (forming diploid RJ711). *MATa mmm2::LEU2* strain RJ713 was isolated after sporulation of the diploid. *mmm1::URA3 mmm2::LEU2* strain RJ797 was formed as follows. First, *MMM2/mmm2::LEU2* strain RJ711 was transformed with *MMM2-URA3* plasmid pM169 (see below). After sporulation, a haploid *mmm2::LEU2* strain with pM169 was isolated and crossed to *mmm1*Δ strain YSB120. After plasmid loss and sporulation, *mmm1::URA3 mmm2::LEU2* strain RJ797was isolated. RJ892, which expresses Mmm2p-HA, was constructed by integrating plasmid pMS20 (see below) at *MMM2* by homologous recombination in strain YPH250. *MMM1::GFP-HIS3* strain SS12, which expresses an Mmm1p-GFP fusion protein, was constructed by PCR-mediated gene replacement using the *GFP-HIS3* cassette from pSS5 (see below) and oligos 756 and 757 in strain FY833. Similarly, *MMM2::GFP-HIS3* strain MY5, which expresses Mmm2p-GFP was constructed using pSS5 and oligos 1320 and 1321, and a second round of PCR amplification using oligos 1322 and 1323. *MMM1::GFP-HIS3 mmm2::kanMX4* strain AAH4 was generated by PCR-mediated gene replacement, using the *kanMX4* drug resistance marker from pRS400 (Brachmann et al., 1998), oligos 154 and 155, and strain SS12. Likewise, *MMM2::GFP-HIS3 mmm1::kanMX4* strain MY6 was generated using pRS400 and oligos 313 and 314. *MMM1::HA MMM2::myc* strain RJ1719 was constructed using protease-deficient strain BJ2168 (Jones, 1991), pFA6a-3HA-TRP1, and pFA6a-13Myc-kanMX6 as previously described (Longtine et al., 1998). *ugo1*Δ *fzo1*Δ strain RJ1302 was made by crossing *fzo1*Δ strain YHS75 (Sesaki et al., 2003) with HA-Fzo1p–containing plasmid pHS72 (Sesaki and Jensen, 2001) to *ugo1*Δ strain YHS72 (Sesaki and Jensen, 2001) with myc-Ugo1p–expressing plasmid pHS78 (see below). Standard yeast media and molecular genetic techniques were used (Adams et al., 1997).

Plasmid constructs

pSB201, which carries *MMM1* on a 2μ-*URA3-ADE2* plasmid, was constructed by PCR amplifying *MMM1* using oligonucleotides 113 and 118. The *MMM1*-containing fragment was blunt-end ligated into the EcoRV site of Bluescript SK II+ (Stratagene), forming pSB201C. A BamHI-XhoI fragment containing *MMM1* was isolated from pSB201C and inserted into BamHI-XhoI–cut pRS426 (Sikorski and Hieter, 1989), forming pSB201A. A BamHI fragment containing the *ADE2* gene from pDK301 (a gift from D. Koshland, Carnegie Institute, Baltimore, MD) was then cloned into the BamHI site of pSB201A, forming pSB201.

pSB209, which carries an insertion of *LEU2* in the *MMM2* open reading frame, was constructed as follows. First, pSB202, which carries *MMM2* on a 2-kbp PstI fragment in pRS200 (Sikorski and Hieter, 1989), was digested with NsiI and the DNA ends filled in with Klenow polymerase. Next, a 4-kbp PstI fragment carrying *LEU2* was isolated from YEp13 (Broach et al., 1979), the DNA ends made blunt with Klenow polymerase, and then the fragment was inserted into the filled-in NsiI site of pRS202.

MMM2-containing plasmid pM169 was formed by inserting an XhoI-NotI fragment with *MMM2* from pSB202 into XhoI-NotI–cut pRS316, a *URA3-CEN* plasmid (Sikorski and Hieter, 1989).

Point mutations in *MMM2* and in the overlapping YGL218w ORF were generated by site-directed mutagenesis (Quickchange; Stratagene) of pSB202. Using oligos 1187 and 1188, pMY1 carries a change from G to A at nucleotide 126 in YGL128w, which creates a stop codon in the ORF. This change does not alter the amino acid composition of the *MMM2* ORF (residue 161 remains a leucine). Using oligos 1185 and 1186, pMY2 carries an A to T change at nucleotide 508, creating a stop codon in the *MMM2* ORF. This alteration creates a conservative change (F34Y) in the YGL128w ORF. All changes were verified by DNA sequencing.

pSB16, a *TRP1-CEN* plasmid that carries the Mmm2p-HA fusion protein, was constructed as follows. First, sequences containing the *MMM2* 3′ end were PCR amplified using oligos 20 and 144 and digested with PstI and NotI. *MMM2* coding sequences were amplified with oligos 21 and 145 and digested with NotI and EcoRI. Both fragments were then inserted into PstI-EcoRI–cut pRS314 (Sikorski and Hieter, 1989), forming pSB214. A 900-bp EcoRI fragment with 5′ *MMM2* sequences was isolated from pSB202 and inserted into EcoRI-cut pSB214, forming pSB215. pSB215 contains the complete *MMM2* gene with a NotI site inserted just before its stop codon. To create Mmm2p-HA, a 114-bp NotI fragment with three tandem copies of the influenza HA epitope (Tyers et al., 1992) was inserted into NotI-cut pSB215, yielding pSB216. To make pMS20, a PstI fragment

carrying *MMM2::HA* was isolated from pSB16 and inserted into *LEU2* integrating plasmid pRS205 (Sikorski and Hieter, 1989).

pAAH13, a *TRP1-CEN* plasmid expressing a Mmm2p-GFP fusion protein, was created by inserting a PstI-NotI fragment containing *MMM2* from pSB215 into PstI-NotI–cut pAAH1 (Aiken Hobbs et al., 2001).

pMY3, a *LEU2-CEN* plasmid expressing a Mmm2p-RFP fusion protein, was constructed by first amplifying RFP from pDsRed.T1 (Bevis and Glick, 2002) using oligonucleotides 509 and 575. Next, the PCR product was digested with SacII and NotI and then inserted into SacII-NotI–digested pAAH1, forming pKC15. Finally, *MMM2* was isolated from XhoI-NotI–digested pAAH13 and subcloned into XhoI-NotI–cut pKC15.

pSS5, which carries a *GFP-HIS3* cassette for chromosomal tagging, was made by PCR amplifying the *TIM23* terminator in pAAH3 (Aiken Hobbs et al., 2001) using oligos 573 and 243, and then inserted into SacI-SacII–digested pAAH3, forming pSS6. Next, the *HIS3* gene was amplified from pRS413 (Sikorski and Hieter, 1989) using oligos 654 and 655, and then inserted into SacI-cut pSS6 by recombinational cloning in yeast (Oldenburg et al., 1997), yielding pSS7. Finally, a GFP-containing fragment was isolated from SacII-NotI–digested pAAH1 and inserted into SacII-NotI–cut pSS7.

pHS78, which expresses Ugo1p with the myc epitope at its NH_2 terminus, was constructed by inserting an XhoI-NotI fragment from pHS57 (Sesaki and Jensen, 2001) into XhoI-NotI–cut pRS316.

Isolation of the *mmm2-1* mutant

ade2 ura3 mmm1-1 strain YSB105 carrying the *MMM1-ADE2-URA3* plasmid pSB201 was mutagenized in ethane methyl sulfonate (50 min incubation; 5% cell survival) as previously described (Adams et al., 1997). Cells were plated (600–800 colonies per plate) onto 120 semi-synthetic plates (Adams et al., 1997) containing 2% lactate as the sole carbon source and incubated for 4 wk at 24°C. Mutants unable to lose the *ADE2*-containing pSB201 plasmid were identified as completely white colonies, whereas cells that were not plasmid dependent formed red–white sectored colonies composed of both *ADE2* and *ade2* cells. 200 candidates were initially identified that seemed unable to lose the pSB201 plasmid. The 200 mutants were retested on 5FOA plates (Boeke et al., 1984) for the ability to lose the *URA*3-containing pSB201 plasmid, and 16 potential *mmm1-1* synthetic lethal mutants were isolated. One candidate, called SB8, was chosen for further study. The other 15 mutants include alleles of *MMM1* and *MMM2* and one new, uncharacterized mutant that is currently under investigation.

SB8 was crossed to wild-type strain YPH252, and diploid cells that lost the *MMM1-ADE2-URA3*–containing plasmid were selected on 5FOA medium. Meiotic analysis of the diploid showed that SB8 contained *mmm1-1* and a new mutation, called *mmm2-1*. *mmm1-1 mmm2-1* strain SB9 was formed by plating SB8 cells onto 5FOA medium to select for cells that had lost the *MMM1-ADE2-URA3*–containing plasmid.

Isolation of the MMM2 gene

SB8 cells, *ade2 ura3 mmm1-1 mmm2-1* cells carrying the pSB201 plasmid, were transformed with a genomic DNA library in the *TRP1-CEN* plasmid, pRS200 (Sikorski and Hieter, 1989). Approximately 20,000 Trp^+ transformants were isolated. Plates were replica plated to 5FOA medium at 24°C to select for cells that could lose the *MMM1-ADE2-URA3*–containing pSB201 plasmid. Even though *mmm1-1 mmm2-1* cells can grow on glucose-containing media at 24°C, the growth rate is much slower than *mmm1-1* alone. Since SB8 cells that carry the *MMM1-ADE2-URA3* plasmid are white (*ADE2*) and cells that have lost the plasmid are red (*ade2;* Reaume and Tatum, 1949), colonies that grew well on the 5FOA plates (13 total) were also examined for colony color. The library plasmid from three red colonies was isolated (Hoffman and Winston, 1987). Two of the plasmids were found to carry *MMM1*, while the third (pSB200) contained a DNA insert from chromosome VII. pSB202, which carries a 2.1-kbp PstI fragment from pSB200 inserted into *CEN-TRP1* plasmid pRS200 (Sikorski and Hieter, 1989), was shown to completely rescue the synthetic lethal growth defect of *mmm1-1 mmm2-1* cells.

The DNA insert of pSB202 was found to carry two overlapping genes, YGL218w and YGL219c. Three approaches were used to show that YGL219c is the *MMM2* gene. (1) Two plasmids, pMY1 and pMY2, were constructed (see above). pMY1 contains an early stop mutation in the YGL218w ORF, but the single base pair alteration does not change the coding of YGL219c. pMY2 carries a stop codon in YGL219c, which makes a conservative change (F34Y) in the YGL218w ORF. We found that pMY2 failed to rescue *mmm2*Δ defect, whereas pMY1 had full *MMM2* function. (2) We found that a 1.2-kbp EcoRI fragment carrying the complete YGL218w ORF, but only part of YGL219c, did not contain *MMM2* function. (3) Indicating that pRS200 contains the actual *MMM2* gene and not an unlinked suppressor, we found that the chromosomal *mmm2::LEU2* disruption created using the cloned DNA was allelic to the *mmm2-1* mutation in genetic crosses.

Subcellular and mitochondrial fractionation

Yeast cells were homogenized and separated into a mitochondrial pellet and a post-mitochondrial supernatant as previously described (Daum et al., 1982), with modifications for growing plasmid-containing cells (Emtage and Jensen, 1993; Burgess et al., 1994). Preparation of mitochondrial membrane vesicles and the separation of outer membrane and inner membrane by sucrose step gradients were as previously described (Aiken Hobbs et al., 2001; Sesaki et al., 2003). To test whether Mmm2p was an integral membrane protein, mitochondria were osmotically shocked and sonicated (Kerscher et al., 1997) and resuspended to 100 μg/ml protein in 0.1 M sodium carbonate, pH 11, or 1.5 M sodium chloride, followed by centrifugation at 40 psi in a Beckmann airfuge for 30 min. For protease studies, mitochondria were treated with 100 μg/ml trypsin (Sigma-Aldrich) for 30 min on ice, followed by the addition of a fivefold molar excess of soybean trypsin inhibitor (Sigma-Aldrich). To disrupt the outer membrane, mitochondria were resuspended in 0.1 M sorbitol; 20 mM Hepes-KOH, pH 7.4, followed by incubation on ice for 30 min. Immunoprecipitations from Triton X-100–solubilized mitochondria were performed as previously described (Sesaki et al., 2003), using mouse 9E10 anti-myc antibodies (Covance).

Proteins were analyzed by SDS-PAGE and Western blotting to Immobilon filters (Millipore) using standard techniques (Current Protocols Online; http://www.mrw2.interscience.wiley.com/cponline). HA-tagged proteins were identified by incubation of filters with mouse ascites fluid prepared using 12CA5 cells (Niman et al., 1983; BABCO). Myc-tagged proteins were visualized using PRB-150 antibodies (Covance). Yeast proteins were identified using antiserum to the β subunit of the F_1-ATPase (a gift from M. Yaffe, University of California, San Diego, CA), Tim23p (Emtage and Jensen, 1993), hexokinase (a gift from M. Yaffe), cytochrome b2 (a gift from G. Schatz, Biocenter, Basel, Switzerland), or OM45p (Yaffe et al., 1989). Immune complexes were detected using HRP-conjugated secondary antibody (Amersham Biosciences) followed by chemiluminescence (SuperSignal; Pierce Chemical Co.). Western blots were quantitated using Quantity One® software (Bio-Rad Laboratories).

Fluorescence microscopy

Cells were grown at 30°C to mid-log phase (OD_{600} = 0.5–1.0) in YEP or SD medium containing either 2% galactose or 2% raffinose, supplemented with the appropriate amino acids. To stain mitochondria, cells were incubated with 0.1 μM MitoTracker™ CMX-Ros (Molecular Probes) for 30 min, or examined immediately after staining with 100 ng/ml 3,3′dihexyloxacarbocyanine ($DiOC_6$; Molecular Probes) or 2 μM MitoFlour 589 (Molecular Probes). To stain mtDNA, cells were incubated with 1 μg/ml DAPI (Molecular Probes) for 15 min. Cells were examined with a Carl Zeiss MicroImaging, Inc. Axioscop microscope using a 100X plan apochromat objective lens equipped with differential interference contrast (DIC) optics. Images were captured with an Orca ER CCD camera (Hamamatsu Corp.) using Openlab software, version 3.0.8 (Improvision). Alternatively, cells were imaged using a DeltaVision system (Applied Precision Instruments) based on an Olympus microscope with a 100X plan apochromat objective and a PXL CCD camera (Roper Industries). Images in the z-axis were taken every 0.2 μm over ∼4–6 μm, and each image was deconvolved using DeltaVision software. For 3D reconstructions, all images were used; for figures, the indicated number of images were compressed.

Gel filtration analysis

Mitochondria (1.0 mg protein) from protease-deficient strain BJ2168 (Jones, 1991) were solubilized in digitonin buffer (1% digitonin, 150 mM KOAc, 30 mM Hepes-KOH, pH 7.4) containing a 1:100 dilution of protease inhibitor cocktail (P-8340; Sigma-Aldrich). After centrifugation at 45,000 rpm for 30 min, the supernatant was loaded onto a Superdex 200 column (Amersham Biosciences) equilibrated with digitonin buffer containing 0.5% digitonin. Fractions (0.5 ml) were collected and analyzed by Western blotting. Molecular mass standards (thyroglobulin, 667 kD; ferritin, 440 kD; catalase, 232 kD; lactate dehydrogenase, 140 kD; bovine serum albumin, 67 kD; Amersham Biosciences) were run under identical conditions.

Quantitation of mtDNA

Total yeast DNA was isolated, dot-blotted to nylon membranes, and probed with ^{32}P-labeled mitochondrial *COX2* and nuclear *TIM23* genes as previously described (Aiken Hobbs et al., 2001). Probes were made using Ready-to-Go DNA™ labeling beads (Amersham Biosciences). Membranes

were analyzed by phosphorimaging using a Bio-Rad Laboratories Molecular Imager® FX and quantitated using Quantity One® software (Bio-Rad Laboratories). All *COX2* values were normalized to the amount of hybridization to *TIM23*.

Production of Mmm2p and Mmm1p antibodies

Peptides corresponding to the COOH terminus of Mmm1p (CKNTREEKPTEL; Johns Hopkins Biosynthesis & Sequencing Facility) or Mmm2p (CWKWGMEDSPPPYH; Boston Biomolecules) were synthesized and coupled to keyhole limpet hemocyanin as previously described (Doolittle, 1986). A terminal cysteine residue was added to facilitate coupling of each peptide. Keyhole limpet hemocyanin–conjugated peptides were then injected into rabbits for antiserum production (Covance). Affinity purification of Mmm1p antibodies using the COOH-terminal peptides coupled to beads (Reduce-Imm Reducing Kit and SulfoLink Kit; Pierce Chemical Co.) followed the manufacturers' directions, except that antibodies were eluted with 4 M magnesium chloride and dialyzed against PBS.

Online supplemental material

Fig. S1 shows that *mmm2*Δ mutants contain normal actin distribution and ER organization. Fig. S2 shows that *mmm2*Δ *mdm10*Δ double mutants are similar to either the *mmm2*Δ or *mdm10*Δ mutants alone. Fig. S2 also shows that *mmm2*Δ *dnm1*Δ double mutants and *mmm2*Δ *fzo1*Δ double mutants are intermediate in phenotype compared with the *mmm2*Δ, *dnm1*Δ, or *fzo1*Δ single mutants. The supplemental material is available at http://www.jcb.org/cgi/content/full/jcb.200308012/DC1.

We especially thank Doug Robinson and Rosemary Stuart for their assistance with our gel filtration studies, Hiromi Sesaki for help with immunoprecipitations, Ben Glick (University of Chicago, Chicago, IL) for pDsRed.T1, Sheryl Southard (Johns Hopkins University School of Medicine) for the *GFP-HIS3* cassette, and Doug Koshland for the *ADE2* plasmid. We would also like to thank Kara Cerveny, Cory Dunn, Heidi Hoard-Fruchey and Hiromi Sesaki for comments on the manuscript.

This work was supported by grant R01-GM54021 from the United States Public Health Service to R.E. Jensen and in part by National Institutes of Health predoctoral training grant 2T32-GM07445 to M. Youngman.

Submitted: 4 August 2003
Accepted: 15 January 2004

References

Adams, A., D. Gottschling, C. Kaiser, and T. Stearns. 1997. Methods in yeast genetics. Cold Spring Harbor Laboratory, Cold Spring Harbor, NY. 177 pp.

Aiken Hobbs, A.E., M. Srinivasan, J.M. McCaffery, and R.E. Jensen. 2001. Mmm1p, a mitochondrial outer membrane protein, is connected to mitochondrial DNA (mtDNA) nucleoids and required for mtDNA stability. *J. Cell Biol.* 152:401–410.

Attardi, G., and G. Schatz. 1988. Biogenesis of mitochondria. *Annu. Rev. Cell Biol.* 4:289–333.

Azpiroz, R., and R.A. Butow. 1993. Patterns of mitochondrial sorting in yeast zygotes. *Mol. Biol. Cell.* 4:21–36.

Basson, M.E., R.L. Moore, J. O'Rear, and J. Rine. 1987. Identifying mutations in duplicated functions in *Saccharomyces cerevisiae*: recessive mutations in HMG-CoA reductase genes. *Genetics.* 117:645–655.

Bender, A., and J.R. Pringle. 1991. Use of a screen for synthetic lethal and multicopy suppressee mutants to identify two new genes involved in morphogenesis in *Saccharomyces cerevisiae*. *Mol. Cell. Biol.* 11:1295–1305.

Berger, K.H., L.F. Sogo, and M.P. Yaffe. 1997. Mdm12p, a component required for mitochondrial inheritance that is conserved between budding and fission yeast. *J. Cell Biol.* 136:545–553.

Berthold, J., M.F. Bauer, H.C. Schneider, C. Klaus, K. Dietmeier, W. Neupert, and M. Brunner. 1995. The MIM complex mediates preprotein translocation across the mitochondrial inner membrane and couples it to the mt-Hsp70/ATP driving system. *Cell.* 81:1085–1093.

Bevis, B.J., and B.S. Glick. 2002. Rapidly maturing variants of the *Discosoma* red fluorescent protein (DsRed). *Nat. Biotechnol.* 20:83–87.

Boeke, J.D., F. LaCroute, and G.R. Fink. 1984. A positive selection for mutants lacking orotidine-5′-phosphate decarboxylase activity in yeast: 5-fluoro-orotic acid resistance. *Mol. Gen. Genet.* 197:345–346.

Boldogh, I.R., D.W. Nowakowski, H.C. Yang, H. Chung, S. Karmon, P. Royes, and L.A. Pon. 2003. A protein complex containing Mdm10p, Mdm12p, and Mmm1p links mitochondrial membranes and DNA to the cytoskeleton-based segregation machinery. *Mol. Biol. Cell.* 14:4618–4627.

Brachmann, C.B., A. Davies, G.J. Cost, E. Caputo, J. Li, P. Hieter, and J.D. Boeke. 1998. Designer deletion strains from *Saccharomyces cerevisiae* 288C: a useful set of strains and plasmids for PCR-mediated gene disruption and other applications. *Yeast.* 14:115–132.

Broach, J.R., J.N. Strathern, and J.B. Hicks. 1979. Transformation in yeast: development of a hybrid cloning vector and isolation of the CAN1 gene. *Gene.* 8:121–133.

Burgess, S.M., M. Delannoy, and R.E. Jensen. 1994. MMM1 encodes a mitochondrial outer membrane protein essential for establishing and maintaining the structure of yeast mitochondria. *J. Cell Biol.* 126:1375–1391.

Daum, G., P.C. Böhni, and G. Schatz. 1982. Import of proteins into mitochondria. Cytochrome b2 and cytochrome c peroxidase are located in the intermembrane space of yeast mitochondria. *J. Biol. Chem.* 257:13028–13033.

Dekker, P.J., H. Muller, J. Rassow, and N. Pfanner. 1996. Characterization of the preprotein translocase of the outer mitochondrial membrane by blue native electrophoresis. *Biol. Chem.* 377:535–538.

Dekker, P.J., F. Martin, A.C. Maarse, U. Bomer, H. Muller, B. Guiard, M. Meijer, J. Rassow, and N. Pfanner. 1997. The Tim core complex defines the number of mitochondrial translocation contact sites and can hold arrested preproteins in the absence of matrix Hsp70-Tim44. *EMBO J.* 16:5408–5419.

Dimmer, K.S., S. Fritz, F. Fuchs, M. Messerschmitt, N. Weinbach, W. Neupert, and B. Westermann. 2002. Genetic basis of mitochondrial function and morphology in *Saccharomyces cerevisiae*. *Mol. Biol. Cell.* 13:847–853.

Doolittle, R.F. 1986. Of URFs and ORFs: A Primer on How to Analyze Derived Amino Acid Sequences. University Science Books, Mill Valley, CA. 103 pp.

Drubin, D.G., H.D. Jones, and K.F. Wertman. 1993. Actin structure and function: roles in mitochondrial organization and morphogenesis in budding yeast and identification of the phalloidin-binding site. *Mol. Biol. Cell.* 4:1277–1294.

Emtage, J.L., and R.E. Jensen. 1993. MAS6 encodes an essential inner membrane component of the yeast mitochondrial protein import pathway. *J. Cell Biol.* 122:1003–1012.

Forte, M., H.R. Guy, and C.A. Mannella. 1987. Molecular genetics of the VDAC ion channel: structural model and sequence analysis. *J. Bioenerg. Biomembr.* 19:341–350.

Hermann, G.J., E.J. King, and J.M. Shaw. 1997. The yeast gene, MDM20, is necessary for mitochondrial inheritance and organization of the actin cytoskeleton. *J. Cell Biol.* 137:141–153.

Hermann, G.J., J.W. Thatcher, J.P. Mills, K.G. Hales, M.T. Fuller, J. Nunnari, and J.M. Shaw. 1998. Mitochondrial fusion in yeast requires the transmembrane GTPase Fzo1p. *J. Cell Biol.* 143:359–373.

Hoffman, C.S., and F. Winston. 1987. A ten-minute DNA preparation from yeast efficiently releases autonomous plasmids for transformation into *Escherichia coli*. *Gene.* 57:267–272.

Jones, E.W. 1991. Tackling the protease problem in *Saccharomyces cerevisiae*. *Methods Enzymol.* 194:428–453.

Kerscher, O., J. Holder, M. Srinivasan, R.S. Leung, and R.E. Jensen. 1997. The Tim54p-Tim22p complex mediates insertion of proteins into the mitochondrial inner membrane. *J. Cell Biol.* 139:1663–1675.

Kondo-Okamoto, N., J.M. Shaw, and K. Okamoto. 2003. Mmm1p spans both the outer and inner mitochondrial membranes and contains distinct domains for targeting and foci formation. *J. Biol. Chem.* 278:48997–49005.

Longtine, M.S., A. McKenzie, III, D.J. Demarini, N.G. Shah, A. Wach, A. Brachat, P. Philippsen, and J.R. Pringle. 1998. Additional modules for versatile and economical PCR-based gene deletion and modification in *Saccharomyces cerevisiae*. *Yeast.* 14:953–961.

McConnell, S.J., and M.P. Yaffe. 1992. Nuclear and mitochondrial inheritance in yeast depends on novel cytoplasmic structures defined by the MDM1 protein. *J. Cell Biol.* 118:385–395.

Meeusen, S., and J. Nunnari. 2003. Evidence for a two membrane-spanning autonomous mitochondrial DNA replisome. *J. Cell Biol.* 163:503–510.

Messerschmitt, M., S. Jakobs, F. Vogel, S. Fritz, K.S. Dimmer, W. Neupert, and B. Westermann. 2003. The inner membrane protein Mdm33 controls mitochondrial morphology in yeast. *J. Cell Biol.* 160:553–564.

Miyakawa, I., H. Aoi, N. Sando, and T. Kuroiwa. 1984. Fluorescence microscopic studies of mitochondrial nucleoids during meiosis and sporulation in the yeast, *Saccharomyces cerevisiae*. *J. Cell Sci.* 66:21–38.

Miyakawa, I., N. Sando, S. Kawano, S. Nakamura, and T. Kuroiwa. 1987. Isolation of morphologically intact mitochondrial nucleoids from the yeast, *Saccharomyces cerevisiae*. *J. Cell Sci.* 88(Pt 4):431–439.

Newman, S.M., O. Zelenaya-Troitskaya, P.S. Perlman, and R.A. Butow. 1996. Analysis of mitochondrial DNA nucleoids in wild-type and a mutant strain of *Saccharomyces cerevisiae* that lacks the mitochondrial HMG box protein Abf2p. *Nucleic Acids Res.* 24:386–393.

Niman, H.L., R.A. Houghten, L.E. Walker, R.A. Reisfeld, I.A. Wilson, J.M. Hogle, and R.A. Lerner. 1983. Generation of protein-reactive antibodies by short peptides is an event of high frequency: implications for the structural basis of immune recognition. *Proc. Natl. Acad. Sci. USA.* 80:4949–4953.

Oldenburg, K.R., K.T. Vo, S. Michaelis, and C. Paddon. 1997. Recombination-mediated PCR-directed plasmid construction in vivo in yeast. *Nucleic Acids Res.* 25:451–452.

Paumard, P., J. Vaillier, B. Coulary, J. Schaeffer, V. Soubannier, D.M. Mueller, D. Brethes, J.P. di Rago, and J. Velours. 2002. The ATP synthase is involved in generating mitochondrial cristae morphology. *EMBO J.* 21:221–230.

Prinz, W.A., L. Grzyb, M. Veenhuis, J.A. Kahana, P.A. Silver, and T.A. Rapoport. 2000. Mutants affecting the structure of the cortical endoplasmic reticulum in *Saccharomyces cerevisiae*. *J. Cell Biol.* 150:461–474.

Reaume, S.E., and E.L. Tatum. 1949. Spontaneous and nitrogen mustard-induced nutritional deficiencies in *Saccharomyces cerevisiae*. *Arch. Biochem.* 22:331–338.

Sesaki, H., and R.E. Jensen. 1999. Division versus fusion: Dnm1p and Fzo1p antagonistically regulate mitochondrial shape. *J. Cell Biol.* 147:699–706.

Sesaki, H., and R.E. Jensen. 2001. UGO1 encodes an outer membrane protein required for mitochondrial fusion. *J. Cell Biol.* 152:1123–1134.

Sesaki, H., S.M. Southard, M.P. Yaffe, and R.E. Jensen. 2003. Mgm1p, a dynamin-related GTPase, is essential for fusion of the mitochondrial outer membrane. *Mol. Biol. Cell.* 14:2342–2356.

Sherratt, D.J. 2003. Bacterial chromosome dynamics. *Science.* 301:780–785.

Sikorski, R., and J.D. Boeke. 1991. *In vitro* mutagenesis and plasmid shuffling: from cloned gene to mutant yeast. *Methods Enzymol.* 194:302–318.

Sikorski, R.S., and P. Hieter. 1989. A system of shuttle vectors and yeast host strains designed for efficient manipulation of DNA in *Saccharomyces cerevisiae*. *Genetics.* 122:19–27.

Sogo, L.F., and M.P. Yaffe. 1994. Regulation of mitochondrial morphology and inheritance by Mdm10p, a protein of the mitochondrial outer membrane. *J. Cell Biol.* 126:1361–1373.

Tandler, B., and C.L. Hoppel. 1972. Mitochondria. Academic Press, New York. 59 pp.

Thorsness, P.E., K.H. White, and T.D. Fox. 1993. Inactivation of YME1, a member of the ftsH-SEC18-PAS1-CDC48 family of putative ATPase-encoding genes, causes increased escape of DNA from mitochondria in *Saccharomyces cerevisiae*. *Mol. Cell. Biol.* 13:5418–5426.

Tyers, M., G. Tokiwa, R. Nash, and B. Futcher. 1992. The Cln3-Cdc28 kinase complex of *S. cerevisiae* is regulated by proteolysis and phosphorylation. *EMBO J.* 11:1773–1784.

Yaffe, M.P., R.E. Jensen, and E.C. Guido. 1989. The major 45-kDa protein of the yeast mitochondrial outer membrane is not essential for cell growth or mitochondrial function. *J. Biol. Chem.* 264:21091–21096.